

RESEARCH ARTICLE

Laser capture microdissection in combination with mass spectrometry: Approach to characterization of tissue-specific proteomes of *Eudiplozoon nipponicum* (Monogenea, Polyopisthocotylea)

Pavel Roudnický^{1*}, David Potěšil², Zbyněk Zdráhal^{2,3}, Milan Gelnar¹, Martin Kašný¹

1 Department of Botany and Zoology, Faculty of Science, Masaryk University, Brno, Czech Republic, **2** Central European Institute of Technology, Masaryk University, Brno, Czech Republic, **3** National Centre for Biomolecular Research, Faculty of Science, Masaryk University, Brno, Czech Republic

* p.roudnický@mail.muni.cz



OPEN ACCESS

Citation: Roudnický P, Potěšil D, Zdráhal Z, Gelnar M, Kašný M (2020) Laser capture microdissection in combination with mass spectrometry: Approach to characterization of tissue-specific proteomes of *Eudiplozoon nipponicum* (Monogenea, Polyopisthocotylea). PLoS ONE 15(6): e0231681. <https://doi.org/10.1371/journal.pone.0231681>

Editor: Matthew Bogyo, Stanford University, UNITED STATES

Received: March 27, 2020

Accepted: May 25, 2020

Published: June 17, 2020

Copyright: © 2020 Roudnický et al. This is an open access article distributed under the terms of the [Creative Commons Attribution License](https://creativecommons.org/licenses/by/4.0/), which permits unrestricted use, distribution, and reproduction in any medium, provided the original author and source are credited.

Data Availability Statement: Proteomic data are now publicly available from PRIDE under accession number: PXD017275. (<https://www.ebi.ac.uk/pride/archive/projects/PXD017275>).

Funding: This work was supported by the Czech Science Foundation (GBP505/12/G112, GAP506/12/1258) and Grant Agency of Masaryk University (MUNI/A/0918/2018). We acknowledge the CF Genomics CEITEC MU supported by the NCMG research infrastructure (LM2018132 funded by

Abstract

Eudiplozoon nipponicum (Goto, 1891) is a hematophagous monogenean ectoparasite which inhabits the gills of the common carp (*Cyprinus carpio*). Heavy infestation can lead to anemia and in conjunction with secondary bacterial infections cause poor health and eventual death of the host. This study is based on an innovative approach to protein localization which has never been used in parasitology before. Using laser capture microdissection, we dissected particular areas of the parasite body without contaminating the samples by surrounding tissue and in combination with analysis by mass spectrometry obtained tissue-specific proteomes of tegument, intestine, and parenchyma of our model organism, *E. nipponicum*. We successfully verified the presence of certain functional proteins (e.g. cathepsin L) in tissues where their presence was expected (intestine) and confirmed that there were no traces of these proteins in other tissues (tegument and parenchyma). Additionally, we identified a total of 2,059 proteins, including 72 peptidases and 33 peptidase inhibitors. As expected, the greatest variety was found in the intestine and the lowest variety in the parenchyma. Our results are significant on two levels. Firstly, we demonstrated that one can localize all proteins in one analysis and without using laboratory animals (antibodies for immunolocalization of single proteins). Secondly, this study offers the first complex proteomic data on not only the *E. nipponicum* but within the whole class of Monogenea, which was from this point of view until recently neglected.

Introduction

Laser-capture microdissection (LCM) was developed as a powerful and reliable tool to overcome the heterogeneity of specimen [1]. It enables isolation of specific tissues, individual cells, or even individual organelles from complex samples based on cell morphology [2,3]. The

MEYS CR) for their support with obtaining scientific data presented in this paper. CIISB research infrastructure project LM2018127 funded by MEYS CR is gratefully acknowledged for their financial support of LC-MS/MS measurements at the Proteomics Core Facility. The work was supported by the project CEITEC 2020 (LQ1601), MEYS CR. Computational resources were supplied by the project "e-Infrastruktura CZ" (e-INFRA LM2018140) provided within the program Projects of Large Research, Development, and Innovations Infrastructures. The funders had no role in study design, data collection and analysis, decision to publish, or preparation of the manuscript.

Competing interests: The authors have declared that no competing interests exist.

method was first described in the second half of the 20th century and since then further developed and modified [2,4–7]. Nowadays, LCM combines laser excision with high-resolution microscopic control, which makes it possible to precisely capture for instance individual cells or even only nucleus while keeping track of the location and morphology of the source tissue [2,3,8].

LCM technology has been used in a wide variety of applications with focus on genomic, transcriptomic, and even proteomic analyses, such as dissection of polar bodies from oocytes for pre-fertilization genetic diagnosis [9], transcriptome-wide analysis of blood vessels from human skin and wound-edge tissue [10], proteomic profiling of dentoalveolar tissues [11], and many other areas [12–14]. But only one study so far used a combination of LCM and mass spectrometry (MS) to localize unique proteins, potential biomarkers, when dealing with the heterogeneity of breast tumor [15].

LCM has also been used in parasitology, especially in sample preparation. Recent studies employed this method in genome sequencing of *Plasmodium relictum*, where it was used to dissect the parasite from infected erythrocytes while excluding the host nucleus [16]. It has also been recently applied in transcriptomic analysis of *Plasmodium cynomolgi* to dissect hypnozoites from hepatocytes [17], in molecular analysis of *Henneguya adiposa* from the fins of catfish [18], and in investigation of ferritin gene expression in vitelline cells and tissue-specific gene profiling (gastrodermis, vitelline, and ovary tissue) of *Schistosoma japonicum* [19,20] and *Schistosoma mansoni* [21,22]. In a study focused on changes in protein composition in intermediate snail host, infected or uninfected by *S. mansoni*, the method was used to dissect hemocytes and sporocysts [23]. So far, however, this technique has not been applied to protein localization, although analysis of tissue-specific proteomes could be an elegant way of localizing the molecules of interest, which would aid a better understanding of their function. It would be faster and less laborious to obtain results this way than by traditional approaches, such as immunolocalization or *in situ* hybridization, which require preparation of recombinant proteins, subsequent immunization processes, and development of RNA-probes.

With respect to investigation of the molecular content of tissue within its morphological context, it was the technique of mass spectrometry imaging (MSI) that made it possible [24]. In parasitology, one study examined chemical markers of the surface of *S. mansoni* by MSI to distinguish between the sexes and the strains [25], while another study dealt with the same organism and investigated the composition of internal organs by histological sections [26]. Because of the technical limits of MSI, the focus was in both cases on the relatively small molecules of triacylglycerols and phosphatidylcholines, not on proteins. This demonstrates why we opted for a different approach: MSI is well-suited to the investigation of small molecules but lacks the ability to identify proteins whose size exceeds app. 15 or 25 kDa [27,28], depending on the specific instrumental setup.

The ability to capture higher molecular weights is essential in search for functional proteins, because their weight usually ranges around several tens of kilodaltons. For example, the digestive peptidases of *E. nipponicum*, such as like cathepsins L and B, have molecular weight of ~25 kDa, ~29 kDa, respectively [29], while one of the serine peptidase inhibitors from the same organism has molecular weight of ~45 kDa [30].

In the present study, our aim is first of all to investigate the potential of using laser capture microdissection (LCM) and liquid chromatography coupled to tandem mass spectrometry (LC-MS/MS) for protein localization and secondly, to obtain tissue-specific proteomes of our experimental organism *Eudiplozoon nipponicum* Goto, 1891 (Polyopisthocotylea). This monogenean is a common hematophagous ectoparasite which inhabits the gills of the common carp (*Cyprinus carpio*). For this species, as for the whole group of parasitic Monogenea, proteomic but also genomic and transcriptomic data are still scarce. In particular, no comprehensive

proteomic or secretomic data have so far been published at all and transcriptomic data are available only for *Neobenedenia melleni* (available in the NCBI BioSample database, <http://www.ncbi.nlm.nih.gov/biosample/>, accession number SAMN00169373). With respect to genomic data, the situation is somewhat better but only two complete genomes are available, namely those of *Gyrodactylus salaris* [31] and *Protopolystoma xenopodis* (available in the NCBI BioProject database, <https://www.ncbi.nlm.nih.gov/bioproject/>, accession number PRJEB1201). For some monogenean species, mitochondrial genomes have, however, been mapped: *N. melleni* [32], *G. salaris* [33], *Gyrodactylus thymalli* [34], *Pseudochauhannea macrochis* [35], *Benedenia hoshinai* [36], *Benedenia humboldti* [37], *Paratetraonchoides inermis* [38], *Lamellogadus spari* and *Lepidotrema longipenis* [39], and *Thaparocleidus asoti* and *T. varicus* [40].

In recent years, this situation started to improve because *E. nipponicum* has been studied in a broader context. Several functional protein molecules of *E. nipponicum* were described [29,30,41–44] and the genome, transcriptome, and secretome of this organism are soon to be published. With this study, we significantly enrich available information on monogenean functional molecular biology by describing protein distribution in selected *E. nipponicum* tissues. Special attention will be paid to peptidases and peptidase inhibitors, which are involved in host–parasite interactions at a molecular level. Our study's aim is to offer new insights into this subject and to suggest some possible directions for future research.

Materials and methods

Parasite material: Collection and fixation

Adults of *E. nipponicum* were collected from freshly sacrificed specimens of *Cyprinus carpio* provided by Rybářství Třeboň a.s., Rybářská 801, Třeboň 379 01, Czech Republic. Isolation and taxonomic identification of the individual worms from the gills was performed as described previously [30].

Extracted worms were thoroughly washed in 10 mM PBS pH 7.2 (PBS) to remove gill tissue debris. Then they were placed in a Petri dish and glass cover placed on them to keep them in stretched flat position. Solution of 4% paraformaldehyde in PBS was pipetted into the Petri dish and the sample was left in room temperature for 4 hrs. After fixation, samples were rinsed with PBS buffer and transferred into cryofixation molds, which were then immersed in OCT compound (Tissue-Tek[®]) and left for 1 hr in room temperature. The molds were then placed in dry ice and frozen blocks stored at -80 °C ([45], modified).

Ethics statement. All procedures performed in studies involving animals were carried out in accordance with European Directive 2010/63/EU and Czech laws 246/1992 and 359/2012 which regulate research involving animals. All experiments were performed with the legal consent of the Animal Care and Use Committee of Masaryk University and of the Research and Development Section of the Ministry of Education, Youth, and Sports of the Czech Republic.

Cryosectioning

The OCT-embedded worms were sectioned in a cryotome (Leica CM1900 UV, -20 °C) in 12 μm thick slices, which were placed on microdissection slides (MembraneSlide 1.0 PEN, Carl Zeiss). Prior the LCM, OCT surrounding the tissues had to be removed, which was achieved by careful dipping of the slides in ddH₂O. In the next step, the tissues were dehydrated by EtOH (96%, two washes for 30 s) and the slides either subjected to LCM immediately or stored in 4 °C for a short time. During cryosectioning, we placed ten to twelve worm sections on a single membrane slide.

Laser capture microdissection

Target tissues were extracted from the histological sections using microdissector PALM MicroBeam (Carl Zeiss) controlled by software PALMRobo 4.6 Pro (Carl Zeiss). Dissected samples were collected into special caps filled with adhesive material for dry collection (AdhesiveCap 500, Carl Zeiss). Cutting options (laser intensity and focus) were adjusted for each type of tissue specifically due to the nature of the parasite body. For each tissue type, areas well defined as to their kind and size were dissected (parenchyma up to 2,000 μm^2 per cut, intestine up to 350 μm^2 per cut, tegument up to 500 μm^2 per cut) with overall area of 1 mm^2 per tissue type. We prepared and analyzed two sets of tissue samples. Each sample was prepared by dissection of an area from a particular tissue from multiple worm individuals.

Sample preparation for LC-MS/MS

Microdissected tissue samples were lysed in SDT buffer (4% SDS, 0.1M DTT, 0.1M Tris/HCl, pH 7.6) in a thermomixer (Eppendorf ThermoMixer[®] C, 30 min, 95°C, 750 rpm). After that, samples were centrifuged (15 min, 20,000 x g) and the supernatant used for filter-aided sample preparation as described elsewhere [46] using 0.5 μg /sample of trypsin (sequencing grade, Promega). Resulting peptides were used for LC-MS/MS analyses. Total peptide amount after sample preparation was estimated using LC-MS analysis on RSLCnano system online coupled with HCTUltra ion trap (Bruker Daltonics) based on the area under the total ion current curve, whereby MEC cell line tryptic digest was used as external calibrant. For final analyses, we used app. 2 μg of tryptic digests.

LC-MS/MS analysis and data evaluation

LC-MS/MS analyses of all peptide mixtures were done using UltiMate™ 3000 RSLCnano system connected to Orbitrap Fusion Lumos Tribrid spectrometer (Thermo Fisher Scientific). Prior to LC separation, tryptic digests were online concentrated and desalted using a trapping column (X-Bridge BEH 130 C18, dimensions 30 mm \times 100 μm , 3.5 μm particles; Waters). After washing the trapping column with 0.1% FA, the peptides were eluted in backflush mode (flow 0.3 $\mu\text{l}/\text{min}$) from the trapping column onto an analytical column (Acclaim Pepmap100 C18, 3 μm particles, 75 μm \times 500 mm; Thermo Fisher Scientific) during a 130 min gradient (1–80% of mobile phase B; mobile phase A: 0.1% FA in water; mobile phase B: 0.1% FA in 80% ACN).

MS data were acquired in a data-dependent mode, selecting up to 20 precursors based on precursor abundance in the survey scan. Resolution of the survey scan was 120,000 (350–2000 m/z) with target value of 4×10^5 ions and maximum injection time of 100 ms. MS/MS spectra were acquired with a target value of 5×10^4 ions (resolution 15,000 at 110 m/z) and maximum injection time of 22 ms. The isolation window for fragmentation was set to 1.2 m/z .

For data evaluation, we used MaxQuant software (v1.6.2.10) [47] with inbuilt Andromeda search engine [48]. Searches against in-house made protein databases were undertaken: *E. nipponicum* (37,076 sequences, manuscript in preparation), *C. carpio* (63,928 sequences, based on <https://www.ncbi.nlm.nih.gov/genome/?term=10839>), and cRAP contaminants (based on <http://www.thegpm.org/crap>). Modifications for all database searches were set as follows: oxidation (M), deamidation (N, Q), and acetylation (Protein N-term) as variable modifications, with carbamidomethylation (C) as a fixed modification. Enzyme specificity was tryptic with two permissible miscleavages. Only peptides and proteins with false discovery rate threshold under 0.01 and proteins with at least two peptide identification were considered. Relative protein abundance was assessed using protein intensities calculated by MaxQuant. For the purpose of this article, protein groups reported by MaxQuant are referred to as proteins. A

complete list of proteins within each protein group can be viewed in the supporting material (S1 Table). Mass spectrometry proteomics data were deposited to the ProteomeXchange Consortium via PRIDE [49] partner repository under dataset identifier PXD017275.

Intensities of reported proteins were further evaluated using software container environment (https://github.com/OmicsWorkflows/KNIME_docker_vnc; version 3.7.1a). Processing workflow is available upon request: it covers decoy hits and removal of contaminant protein groups (cRAP), protein group intensities log₂ transformation and loessF normalization. Carp proteins were filtered out as contaminants. Mapping to *E. nipponicum* transcriptome (accession GFYM00000000.1) was also undertaken, which enriched protein identifications by annotations (GO terms, MEROPS, Pfam and InterPro accessions).

Comparative analyses

Datasets obtained from the three *E. nipponicum* tissues (intestine, parenchyma, and tegument) were compared with each other to identify shared and unique proteins, with special focus on inhibitors and peptidases. Annotations of proteins unique to each tissue were loaded from the Kyoto Encyclopedia of Genes and Genomes (KEGG) while excluding “organismal system” and “human disease” categories [50]. Based on the measured intensity of proteins found in each tissue, the most abundant peptidases and inhibitors were identified using fold change ratios calculated between the respective tissue samples.

Localization of functional proteins

To assess whether our approach could also be applied to protein localization, we compared proteins identified in each tissue with previously characterized proteins whose functions were described in recent publications: cathepsins L and B [29], stefin [43], kunitz [42] and serpin [30].

Results

Laser capture microdissection of tissue samples

We targeted three types of tissue, namely intestine, tegument, and parenchyma (Fig 1). These tissues samples were cut out from 10 μm thick longitudinal cryosections of several individuals of *E. nipponicum*. Total area of each tissue sample was 1 mm², which corresponds to volume of app. 0.012 μm³.

LC-MS/MS analyses and data evaluation

Total peptide yield estimate after filter-aided sample preparation (FASP) showed there were app. 40 μg in intestine, 8 μg in tegument and 6 μg in parenchyma in each dissected tissue type of comparable size, suggesting higher overall protein content in the intestine. In total, i.e. in all three tissues jointly, we identified 2,059 proteins. Of these proteins, 1,978 were found in the intestine, 1,425 in the tegument, and 1,302 in the parenchyma. An overview is listed in Table 1, while Fig 2 shows how many proteins are unique to or shared among the tissues. There were also 273 carp proteins identified, which were filtered out and are not included in the results.

Unique proteins from each tissue were assigned to KEGG pathways (Fig 3). Most annotations turned out to be in the intestine dataset (250 out of 489 entries; 51.1%), followed by the tegument (20 out of 61; 32.8%) and the parenchyma (4 out of 14; 28.6%).

With respect to **peptidases**, we were able to identify 72 in all three tissues jointly. Numbers of peptidases identified in each tissue are shown in the Fig 4. Most peptidases were found in

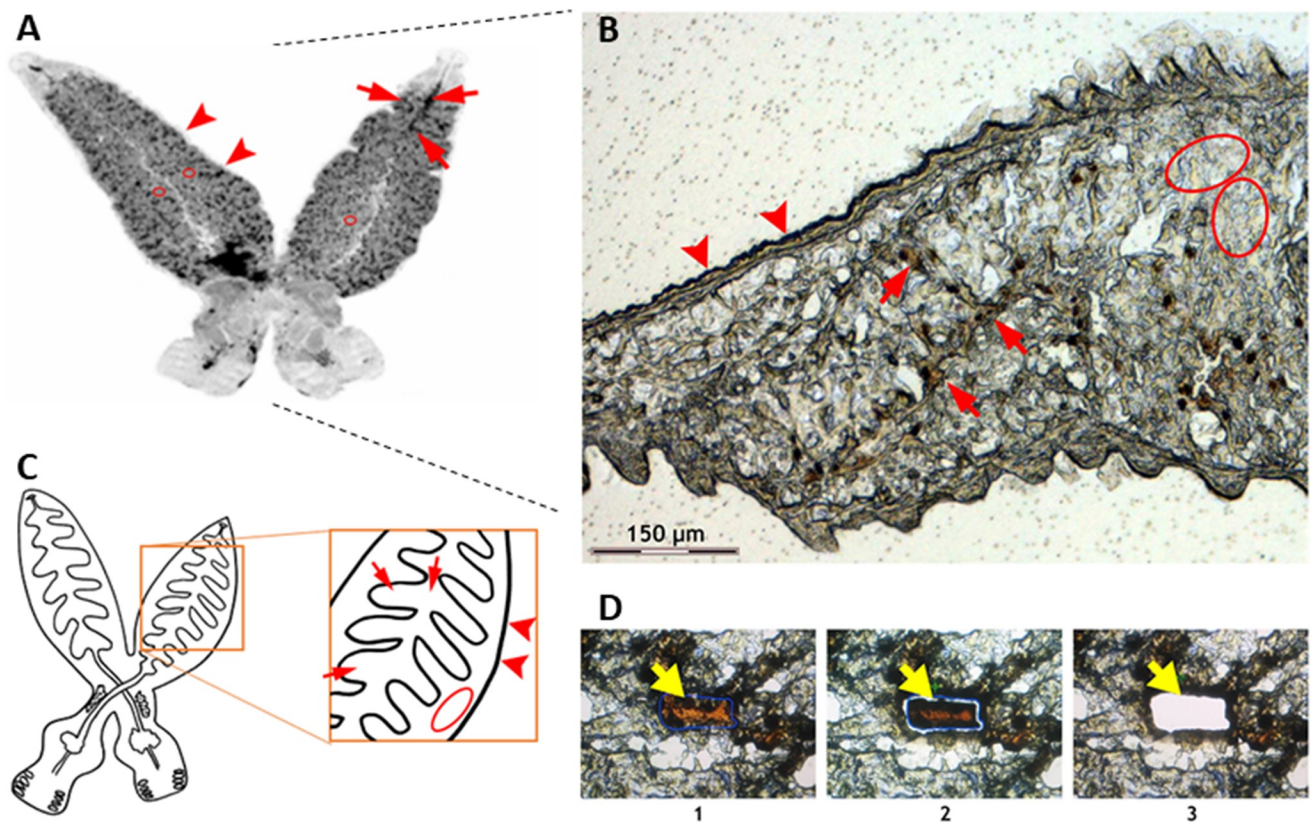


Fig 1. Laser microdissection of chosen tissues of *E. nipponicum*. (A) An overview of *E. nipponicum* body. (B) Part of microdissected section. A branched intestine filled with host blood is clearly visible (red arrow). Tegument is visible at the edge of the section (red arrowhead). Parenchyma is the area with no visible organelles (red ovals). (C) A schematic drawing of worm anatomy and dissected areas. (D) Microdissection process: 1) selection of desired area; 2) laser section; 3) catapulting specimen to collection tube. Yellow arrows point to the dissected area.

<https://doi.org/10.1371/journal.pone.0231681.g001>

the intestine, where one also finds most of the unique ones. Furthermore, we identified 33 **peptidase inhibitors** in all three tissues jointly. Numbers of inhibitors identified in each tissue are shown in Fig 4. Similarly to peptidases, most inhibitors are present in the intestine.

Peptidases unique to a tissue were classified into several groups based on their catalytic mechanism. There are four catalytic groups present in our dataset and only peptidases from the intestine belong to all of them, i.e. to serine, aspartic, cysteine, and metallo. Tegumental peptidases belong to two catalytic groups (serine and metallo), while in the parenchyma, we found no unique peptidases (Fig 5). Unique inhibitors were sorted in several families according to the MEROPS classification (Fig 5). Inhibitors from the intestine were again the most varied ones,

Table 1. Resulting numbers of identified proteins in each tissue.

Tissue	Proteins	Peptidases	Inhibitors
Parenchyma	1,302	52	22
Tegument	1,425	57	24
Intestine	1,978	68	30
Total identifications*	2,059	72	33

*Total identifications refer to all proteins identified in whole dataset including unique and shared proteins among all tissues.

<https://doi.org/10.1371/journal.pone.0231681.t001>

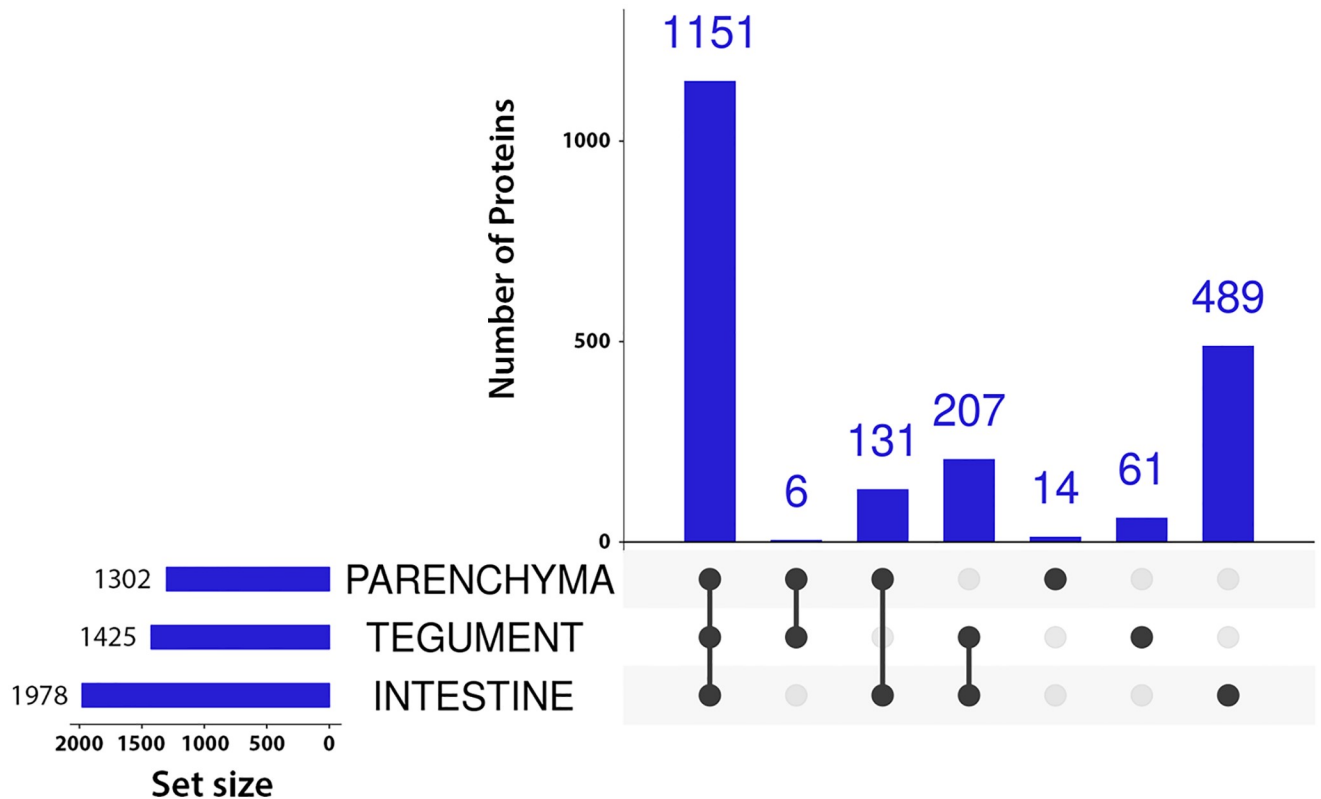


Fig 2. UpSet plot showing numbers of identifications in each tissue. Only proteins identified by ≥ 2 peptides in at least one replicate are considered to be present. Intersections show proteins present in all tissues marked by connected black dots. Black dots without connections refer to proteins unique to that tissue.

<https://doi.org/10.1371/journal.pone.0231681.g002>

covering four (I2, I25, I29, and I32) of the seven families present. In the parenchyma, only one family was present (I4), while tegumental inhibitors belonged to two families (I21 and I87). A list of identifications of unique peptidases and inhibitors can be viewed in [S2 Table](#).

Differently expressed peptidases and inhibitors

Subsequently, we compared the abundance of inhibitors and peptidases in each tissue based on protein intensities. We found three peptidases more abundant in the intestine and four in the tegument. With respect to inhibitors, we found one more abundant in the intestine and one in the parenchyma. For detailed information, see [Table 2](#).

Localization of functional proteins

Seven cathepsins (CL3, CL4, CL6b, c, d, e, and CB) were identified only in the intestine, two (CL1, CL5) in all tissues, and two have not been identified at all although based on a related publication [29], they should be present in the intestine as well. Both inhibitors, i.e. EnStef and EnSerp1, were present in all tissues (see [Table 3](#)).

Discussion

In this study, we report the first tissue-specific proteomic analysis of parasitic monogenean *Eudiplozoon nipponicum*. Using laser capture microdissection, we dissected particular areas of

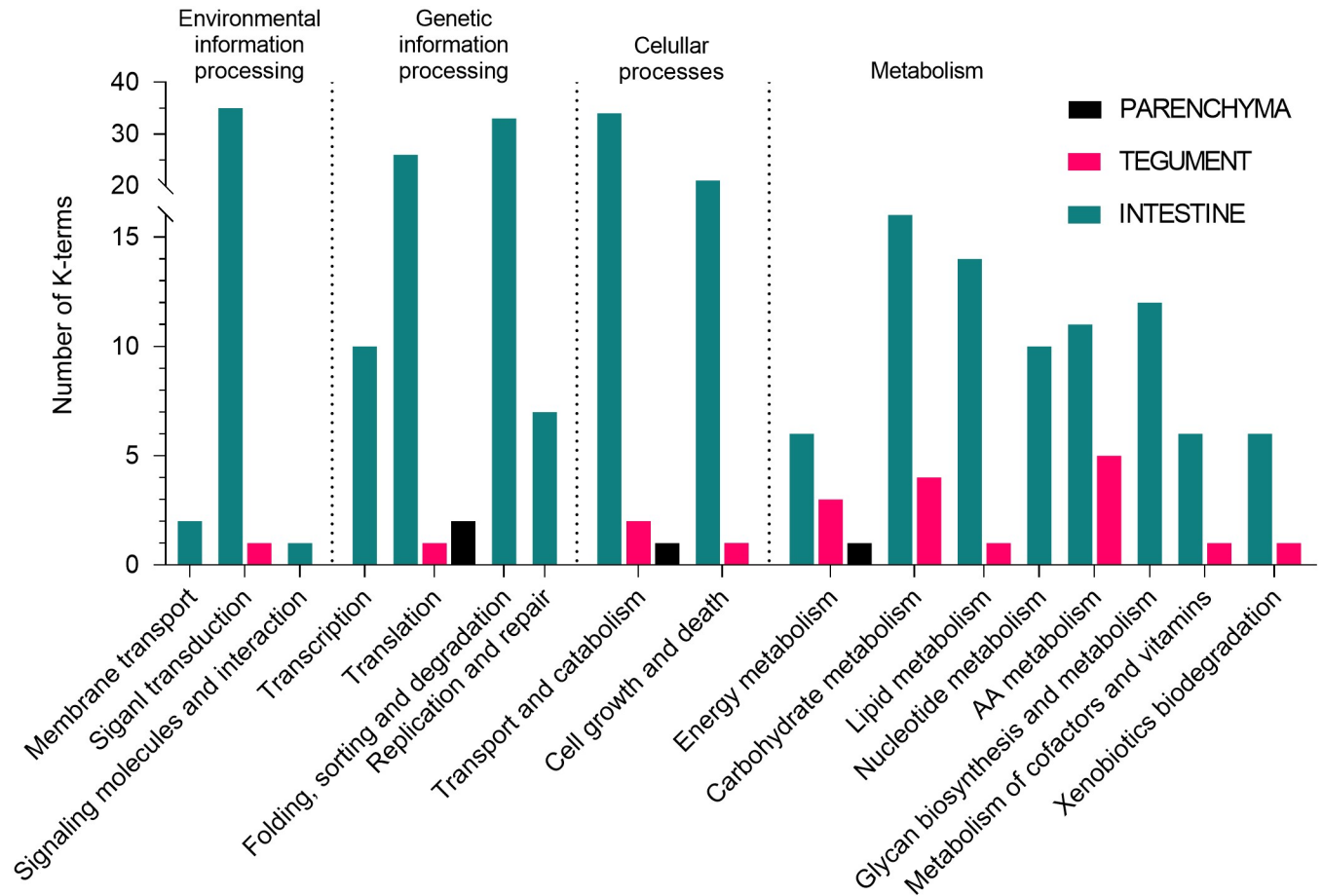


Fig 3. KEGG pathway annotation of the unique proteins from each tissue. Only proteins identified by ≥ 2 peptides in both replicates of a given sample and by ≤ 1 peptide in other samples are considered unique to a sample.

<https://doi.org/10.1371/journal.pone.0231681.g003>

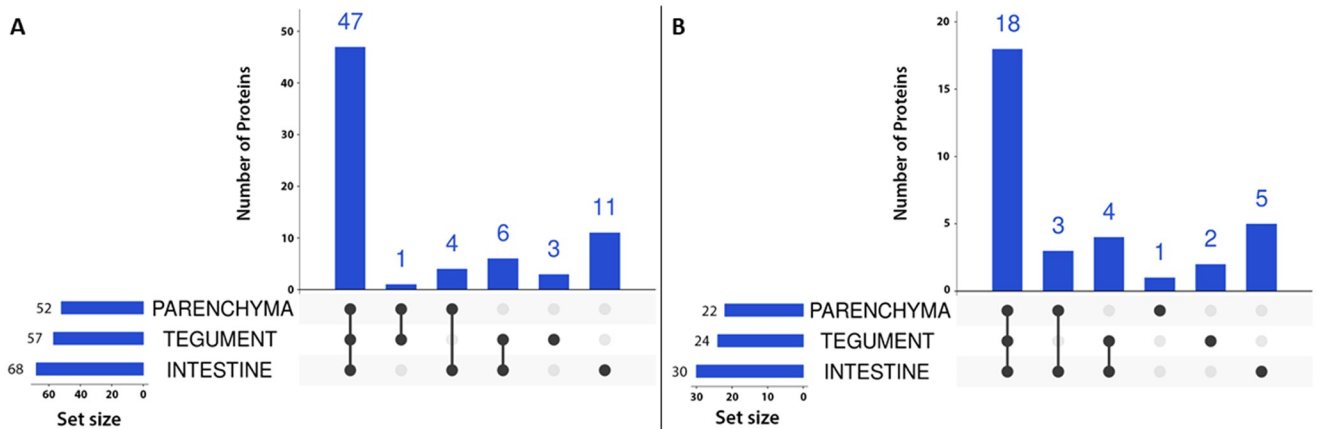


Fig 4. UpSet plots showing the number of peptidases (A) and inhibitors (B) in each tissue. Only proteins identified by ≥ 2 peptides in at least one replicate are considered. Proteins common to several tissues are marked by connected black dots. Black dots without connections refer to proteins unique to that tissue.

<https://doi.org/10.1371/journal.pone.0231681.g004>

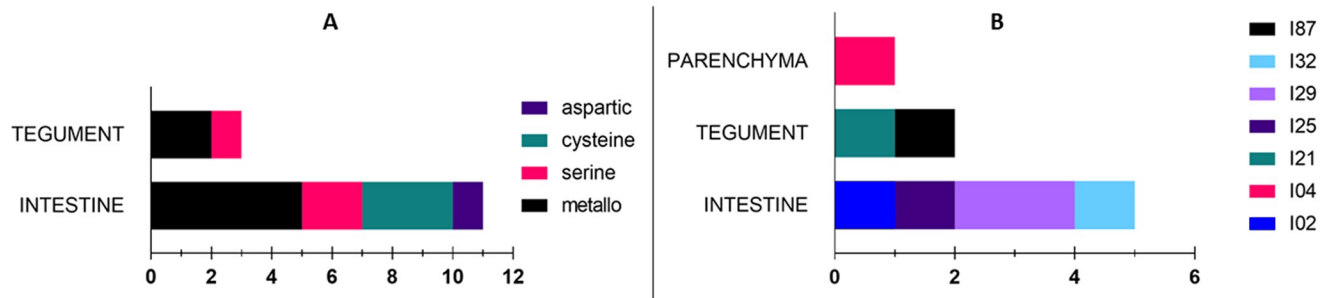


Fig 5. Classification of unique peptidases and inhibitors. (A) Unique peptidases are assigned to groups according to their catalytic type. (B) Similarly, unique inhibitors are sorted into families based on the MEROPS database classification. Only proteins identified by ≥ 2 peptides in both replicates of a sample and by ≤ 1 peptide in other samples are considered unique to a tissue.

<https://doi.org/10.1371/journal.pone.0231681.g005>

three different tissue types of the parasite body and subjected the dissected samples to mass spectrometry-based proteomic analysis. This allowed us to characterize tissue-specific proteomes and to assess the suitability of this approach for proteins tissue-localization. We chose to focus on intestine, tegument, and parenchyma because those tissues can be easily differentiated without any additional histological staining. Moreover, functional proteins from the intestine are of great importance due to their involvement in the host–parasite interplay and a better understanding of these processes could help control not only infections by *E. nipponicum* but possibly by other monogeneans as well. Despite the practical importance of this subject, only a handful of studies so far focused on particular functional proteins [29,30,42–44] and more comprehensive proteomic data were so far missing.

In this study, we identified 2,059 proteins. Most identifications were made in the intestine sample (1,978), less in the tegument (1,425), and the lowest number of identifications was made in the parenchyma (1,302) (Table 1, Fig 2). Of these proteins, 72 (3.50%) were peptidases and 33 (1.60%) inhibitors (Table 1), which is in good agreement with ratios found in other parasites, such as the fluke *S. mansoni* proteome on UniProt (UP000008854, [51]), which contains 6,858 entries and the MEROPS lists 284 (4.14%) peptidases and 129 (1.88%) inhibitors, or the

Table 2. List of the most abundant peptidases and inhibitors.

Protein description	Merops ID	Transcriptome accession	Fold-change*	
			Par. / Int.	Par. / Teg.
More abundant in the parenchyma			Par. / Int.	Par. / Teg.
Family I63 UI	I63.UPW	E_nip_trans_67113_m.419481	7.81	20.30
More abundant in the tegument			Teg. / Int.	Teg. / Par.
Subfamily S1A UP	S01.UPA	E_nip_trans_11554_m.79831	-	18.66
Family M8 UP	M08.UPW	E_nip_trans_09681_m.59668	32.28	10.41
Family M41 UP	M41.UPW	E_nip_trans_12974_m.94993	2.86	18.30
Subfamily S8B UP	S08.UPB	E_nip_trans_69935_m.457916	47.98	-
More abundant in the intestine			Int. / Teg.	Int. / Par.
Carboxypeptidase	S10.002	E_nip_trans_02420_m.6867	22.41	43.50
Family I29 UI	I29.UPW	E_nip_trans_04670_m.20209	3.81	14.67
Family M17 UP	M17.UPW	E_nip_trans_14140_m.106625	11.72	5.95
Family S28 UP	S28.UPW	E_nip_trans_39061_m.265071	13.51	9.50

UI, unassigned peptidase inhibitor; UP, unassigned peptidase.

*Proteins were filtered according to a fold change ≥ 10 . Highlighted values are those which pass this criterion.

<https://doi.org/10.1371/journal.pone.0231681.t002>

Table 3. Localization of functional proteins.

Functional protein	Transcriptome accession	Location
CL1	E_nip_trans_58808_m.372114	P, I, T
CL2	E_nip_trans_70234_m.461805	–
CL3	E_nip_trans_38122_m.258714	I
CL4	E_nip_trans_06099_m.25531	I
CL5	E_nip_trans_65378_m.396731	P, T
CL6a	E_nip_trans_15113_m.115989	–
CL6b	E_nip_trans_04751_m.20488	I
CL6c	E_nip_trans_04670_m.20209	I
CL6d	E_nip_trans_55822_m.362291	I
CL6e	E_nip_trans_60687_m.380367	I
CB	E_nip_trans_02724_m.9562	I
EnStef	E_nip_trans_39617_m.270033	P, I, T
EnSerp1	E_nip_trans_58759_m.402754	P, I, T
EnKT1	E_nip_trans_05461_m.23039; E_nip_trans_00977_m.2066	I

P, parenchyma; I, intestine; T, tegument;–, not identified.

Only identification by ≥ 2 peptides in both replicates was taken into account. Highlighted cells mean consensus of data acquired by LCM + LC-MS/MS with the proposed location in a relevant publication [29].

<https://doi.org/10.1371/journal.pone.0231681.t003>

tick *Ixodes ricinus* proteome (UP000001555, Caler et al. 2008 not published), which contains 20,473 entries and the MEROPS lists 318 (1.55%) peptidases and 277 (1.35%) inhibitors (MEROPS database accessed January 18, 2020). Apart from this, we also identified 273 carp proteins. Vast majority of these were found in the intestine sample set and were related to the food content, as attested by the fact that they included blood proteins (hemoglobin subunits, heme-binding protein, complement factors, antihemorrhagic factor etc.). These proteins were filtered out as expected contaminants.

In terms of tissue specificity of peptidases and inhibitors (Fig 4), the richest environment is the intestine, which is the most metabolically active of the organism: both digestion and nutrient uptake take place in the gut lumen and hematin cells of the gastrodermis [29,52]. The tegument ended up the second, which could be due to the fact that this tissue protects the rest of the body from the environment. It is the site of various important processes, such as glycocalyx maintenance [53,54], sensory perception [55], and secretion [56]. The lowest variety of proteases and inhibitors was found in the parenchyma, where no major organs were dissected. This tissue served primarily as a control for the other two. KEGG pathway annotations provided further support to these conclusions (Fig 3), although the input (unique proteins) for analysis was different for each tissue. Nonetheless, with respect to for instance metabolism, we can conclude that the tegument is much more frequently represented in the particular sections (such as carbohydrate and amino acid metabolism), which may be related to its abovementioned function in surface maintenance. On the other hand, lack of uniqueness in the parenchyma supports our initial expectations, because this tissue provides skeletal and structural support and functions as nutrient transport and storage [57].

Catalytic groups which cover unique identified peptidases are shown in Fig 5. In total, we found representatives of four groups. Most represented were serine, cysteine, and metallopeptidases. This correlates with the number of unique inhibitors, which were assigned to seven families, including representatives of metallo (I87), cysteine (I29, I25, I4), and serine (I4 and

I2) peptidase inhibitors (Fig 5). In all these statistics, the intestine was again dominant with respect to variety. This is once again related to its function, namely feeding, since most peptidases and inhibitors play a role in digestion, inhibition of blood coagulation, and prevention of inflammation [29,42,52].

This expected variety in the intestine is reflected also in the most abundant peptidases/inhibitors (Table 2). For instance, one of the peptidases we found in the intestine was serine carboxypeptidase, whereby serine carboxypeptidases from family S10 are known to have a lysosomal function [58] but it is also assumed they play a role in blood degradation. The latter function seems to be supported by findings on *S. japonicum*, where it has an expression profile similar to the digestive cathepsin [59], while carboxypeptidase, its ortholog from tick *Ixodes ricinus*, has been described as a digestive enzyme [60]. There is also one abundant cysteine peptidase inhibitor from family I29. Its ortholog, a propeptide of *Fasciola hepatica* cathepsin L, proved to be a potent and selective inhibitor which plays a role in cathepsin L maturing and activity regulation [61], which makes its role similar to the *E. nipponicum* cysteine inhibitor.

In the tegument, the most abundant serine peptidase we found belonged to the S8 family of diverse peptidases, most of which play a housekeeping role in protein turnover or processing of precursors of bioactive proteins [62].

In the parenchyma, one functional protein was significantly abundant: an inhibitor from the I63 family. This family contains an inhibitor of metallopeptidase pappalysin-1, which promotes cell growth [63]. We can therefore speculate that the identified inhibitor may play a role in the regulation of a peptidase with similar function.

Moreover, since we have access to the preliminary version of secretome of *E. nipponicum* (manuscript in preparation), we compared our data with it and saw that most secretome proteins are in fact a subset of data obtained in the present study. This is unsurprising because proteins in the secretome are produced by the parasite's glands and intestine and at the time of production, they are situated in the parasite body, which is why they were detected by mass spectrometry in our analysis.

Finally, one of the main goals of this study was to investigate the potential of application of this methodology (LCM + LC-MS/MS) for protein localization. In this approach, one can select just those organs, tissues, or cells one is interested in and they can be extracted cleanly, that is, without contamination by unwanted surrounding tissue. And while this approach also requires further fine-tuning, it is markedly less laborious and time-consuming than the generally used techniques of immunolocalization and *in situ* hybridization [64]. Positive is also the fact that the procedure dispenses with the need to use laboratory animals. In the end, once the analysis is finished, one can go over the list of identified proteins and see where a protein of interest was identified. This can be done repeatedly and for different proteins without the need of additional experiments. The results of this study show that this method confirmed the localization of previously characterized cathepsins and kunitz of *E. nipponicum* [29,42] (Table 3). On the other hand, there is still room for improvement because two of the eleven examined cathepsins were not identified and another two were identified in tissues where they were not expected.

To conclude, our results represent the first tissue-specific proteomic analysis of the monogenean *Eudiplozoon nipponicum*. A combination of techniques, such as laser capture microdissection with subsequent liquid chromatography coupled to tandem mass spectrometry, sheds light on the distribution of functional proteins, including peptidases and inhibitors, within the parenchyma, tegument, and intestine of this parasite. At the same time, the data we obtained represent the first comprehensive proteomic data available for Monogenea, a group of parasites which has so far been, at least in our opinion, neglected.

Supporting information

S1 Table. LC-MS/MS analysis of *E. nipponicum* tissues.

(XLSX)

S2 Table. Unique tissue-specific peptidases and peptidase inhibitors.

(PDF)

Acknowledgments

We would like to thank Anna Pilátová, Ph.D., for English proofreading.

Author Contributions

Conceptualization: Pavel Roudnický, David Potěšil, Martin Kašný.

Data curation: Pavel Roudnický, David Potěšil.

Formal analysis: Pavel Roudnický, David Potěšil.

Funding acquisition: Milan Gelnar.

Investigation: Pavel Roudnický.

Methodology: Pavel Roudnický, Martin Kašný.

Project administration: Zbyněk Zdráhal, Martin Kašný.

Resources: Zbyněk Zdráhal, Milan Gelnar, Martin Kašný.

Supervision: David Potěšil, Martin Kašný.

Visualization: Pavel Roudnický.

Writing – original draft: Pavel Roudnický.

Writing – review & editing: Zbyněk Zdráhal, Martin Kašný.

References

1. Datta S, Malhotra L, Dickerson R, Chaffee S, Sen CK, Roy S. Laser capture microdissection: Big data from small samples. *Histol Histopathol.* 2015; 30: 1255–1269. <https://doi.org/10.14670/HH-11-622> PMID: 25892148
2. Schütze K, Niyaz Y, Stich M, Buchstaller A. Noncontact Laser Microdissection and Catapulting for Pure Sample Capture. *Methods in Cell Biology.* 2007. pp. 647–673. [https://doi.org/10.1016/S0091-679X\(06\)82023-6](https://doi.org/10.1016/S0091-679X(06)82023-6)
3. Espina V, Wulffkuhle JD, Calvert VS, Vanmeter A, Zhou W, Coukos G, et al. Laser-capture microdissection. 2006. <https://doi.org/10.1038/nprot.2006.85> PMID: 17406286
4. Cremer C, Zorn C, Cremer T. An ultraviolet laser microbeam for 257 nm. *Microsc Acta.* 1974; 75: 331–7. PMID: 4599416
5. Berns M, Aist J, Edwards J, Strahs K, Girton J, McNeill P, et al. Laser microsurgery in cell and developmental biology. *Science (80-).* 1981; 213: 505–513. <https://doi.org/10.1126/science.7017933> PMID: 7017933
6. Monajembashi S, Cremer C, Cremer T, Wolfrum J, Greulich KO. Microdissection of human chromosomes by a laser microbeam. *Exp Cell Res.* 1986; 167: 262–265. [https://doi.org/10.1016/0014-4827\(86\)90223-5](https://doi.org/10.1016/0014-4827(86)90223-5) PMID: 3758206
7. Böhm M, Wieland I, Schütze K, Rübber H. Microbeam MOMEt: non-contact laser microdissection of membrane-mounted native tissue. *Am J Pathol.* 1997; 151: 63–7. PMID: 9212732
8. Zhang S, Thakare D, Yadegari R. Laser-Capture Microdissection of Maize Kernel Compartments for RNA-Seq-Based Expression Analysis. In: Lagrimini LM, editor. New York, NY: Springer New York; 2018. pp. 153–163. https://doi.org/10.1007/978-1-4939-7315-6_9

9. Clement-Sengewald A, Buchholz T, Schütze K. Laser Microdissection as a New Approach to Prefertilization Genetic Diagnosis. *Pathobiology*. 2000; 68: 232–236. <https://doi.org/10.1159/000055929> PMID: 11279352
10. Roy S, Patel D, Khanna S, Gordillo GM, Biswas S, Friedman A, et al. Transcriptome-wide analysis of blood vessels laser captured from human skin and chronic wound-edge tissue. *Proc Natl Acad Sci*. 2007; 104: 14472–14477. <https://doi.org/10.1073/pnas.0706793104> PMID: 17728400
11. Salmon CR, Giorgetti APO, Paes Leme AF, Domingues RR, Kolli TN, Foster BL, et al. Microproteome of dentoalveolar tissues. *Bone*. 2017; 101: 219–229. <https://doi.org/10.1016/j.bone.2017.05.014> PMID: 28527949
12. DiIillo M, Pellegrini D, Ait-Belkacem R, De Graaf EL, Caleo M, McDonnell LA. Mass Spectrometry Imaging, Laser Capture Microdissection, and LC-MS/MS of the Same Tissue Section. *J Proteome Res*. 2017; 16: 2993–3001. <https://doi.org/10.1021/acs.jproteome.7b00284> PMID: 28648079
13. Shapiro JP, Biswas S, Merchant AS, Satoskar A, Taslim C, Lin S, et al. A quantitative proteomic workflow for characterization of frozen clinical biopsies: Laser capture microdissection coupled with label-free mass spectrometry. *J Proteomics*. 2012; 77: 433–440. <https://doi.org/10.1016/j.jprot.2012.09.019> PMID: 23022584
14. Nakamura N, Ruebel K, Jin L, Qian X, Zhang H, Lloyd R V. Laser Capture Microdissection for Analysis of Single Cells. 2007. pp. 11–18. https://doi.org/10.1007/978-1-59745-298-4_2 PMID: 17876072
15. Johann DJ, Rodriguez-Canales J, Mukherjee S, Prieto DA, Hanson JC, Emmert-Buck M, et al. Approaching Solid Tumor Heterogeneity on a Cellular Basis by Tissue Proteomics Using Laser Capture Microdissection and Biological Mass Spectrometry †. *J Proteome Res*. 2009; 8: 2310–2318. <https://doi.org/10.1021/pr8009403> PMID: 19284784
16. Lutz HL, Marra NJ, Grewe F, Carlson JS, Palinauskas V, Valkiūnas G, et al. Laser capture microdissection microscopy and genome sequencing of the avian malaria parasite, *Plasmodium relictum*. *Parasitol Res*. 2016; 115: 4503–4510. <https://doi.org/10.1007/s00436-016-5237-5> PMID: 27651044
17. Cubi R, Vembar SS, Biton A, Franetich J-F, Bordessoulles M, Sossau D, et al. Laser capture microdissection enables transcriptomic analysis of dividing and quiescent liver stages of *Plasmodium relapsing* species. *Cell Microbiol*. 2017; 19: e12735. <https://doi.org/10.1111/cmi.12735> PMID: 28256794
18. Stilwell JM, Camus AC, Leary JH, Mohammed HH, Griffin MJ. Molecular confirmation of *Henneguya adiposa* (Cnidaria: Myxozoa) and associated histologic changes in adipose fins of channel catfish, *Ictalurus punctatus* (Teleost). *Parasitol Res*. 2019; 118: 1639–1645. <https://doi.org/10.1007/s00436-019-06295-w> PMID: 30903347
19. Jones MK, McManus DP, Sivadurai P, Glanfield A, Moertel L, Belli SI, et al. Tracking the fate of iron in early development of human blood flukes. *Int J Biochem Cell Biol*. 2007; 39: 1646–1658. <https://doi.org/10.1016/j.biocel.2007.04.017> PMID: 17556009
20. Gobert GN, McManus DP, Nawaratna S, Moertel L, Mulvenna J, Jones MK. Tissue specific profiling of females of *Schistosoma japonicum* by integrated laser microdissection microscopy and microarray analysis. *PLoS Negl Trop Dis*. 2009; 3. <https://doi.org/10.1371/journal.pntd.0000469> PMID: 19564906
21. Nawaratna SSK, McManus DP, Moertel L, Gobert GN, Jones MK. Gene atlas of digestive and reproductive tissues in *Schistosoma mansoni*. *PLoS Negl Trop Dis*. 2011; 5. <https://doi.org/10.1371/journal.pntd.0001043> PMID: 21541360
22. Nawaratna SSK, Gobert GN, Willis C, Chuah C, McManus DP, Jones MK. Transcriptional profiling of the oesophageal gland region of male worms of *Schistosoma mansoni*. *Mol Biochem Parasitol*. 2014; 196: 82–89. <https://doi.org/10.1016/j.molbiopara.2014.08.002> PMID: 25149559
23. Dinguirard N, Cavalcanti MGSS, Wu XJ, Bickham-Wright U, Sabat G, Yoshino TP. Proteomic Analysis of *Biomphalaria glabrata* Hemocytes During in vitro Encapsulation of *Schistosoma mansoni* Sporocysts. *Front Immunol*. 2018; 9: 1–17.
24. Crecelius AC, Schubert US, von Eggeling F. MALDI mass spectrometric imaging meets “omics”: recent advances in the fruitful marriage. *Analyst*. 2015; 140: 5806–5820. <https://doi.org/10.1039/c5an00990a> PMID: 26161715
25. Ferreira MS, de Oliveira DN, de Oliveira RN, Allegretti SM, Vercesi AE, Catharino RR. Mass spectrometry imaging: a new vision in differentiating *Schistosoma mansoni* strains. *J Mass Spectrom*. 2014; 49: 86–92. <https://doi.org/10.1002/jms.3308> PMID: 24446267
26. Kadesch P, Quack T, Gerbig S, Grevelding CG, Spengler B. Lipid Topography in *Schistosoma mansoni* Cryosections, Revealed by Microembedding and High-Resolution Atmospheric-Pressure Matrix-Assisted Laser Desorption/Ionization (MALDI) Mass Spectrometry Imaging. *Anal Chem*. 2019; 91: 4520–4528. <https://doi.org/10.1021/acs.analchem.8b05440> PMID: 30807108
27. Hsu C-C, Chou P-T, Zare RN. Imaging of Proteins in Tissue Samples Using Nanospray Desorption Electrospray Ionization Mass Spectrometry. *Anal Chem*. 2015; 87: 11171–11175. <https://doi.org/10.1021/acs.analchem.5b03389> PMID: 26509582

28. Taverna D, Boraldi F, De Santis G, Caprioli RM, Quaglino D. Histology-directed and imaging mass spectrometry: An emerging technology in ectopic calcification. *Bone*. 2015; 74: 83–94. <https://doi.org/10.1016/j.bone.2015.01.004> PMID: 25595835
29. Jedličková L, Dvořáková H, Dvořák J, Kašný M, Ulrychová L, Vorel J, et al. Cysteine peptidases of *Eudiplozoon nipponicum*: a broad repertoire of structurally assorted cathepsins L in contrast to the scarcity of cathepsins B in an invasive species of haematophagous monogenean of common carp. *Parasit Vectors*. 2018; 11: 142. <https://doi.org/10.1186/s13071-018-2666-2> PMID: 29510760
30. Roudnický P, Vorel J, Ilgová J, Benovics M, Norek A, Jedličková L, et al. Identification and partial characterization of a novel serpin from *Eudiplozoon nipponicum* (Monogenea, Polyopisthocotylea). *Parasite*. 2018; 25: 61. <https://doi.org/10.1051/parasite/2018062> PMID: 30516130
31. Hahn C, Fromm B, Bachmann L. Comparative Genomics of Flatworms (Platyhelminthes) Reveals Shared Genomic Features of Ecto- and Endoparasitic Neodermata. *Genome Biol Evol*. 2014; 6: 1105–1117. <https://doi.org/10.1093/gbe/evu078> PMID: 24732282
32. Zhang J, Wu X, Li Y, Zhao M, Xie M, Li A. The complete mitochondrial genome of *Neobenedenia meleni* (Platyhelminthes: Monogenea): mitochondrial gene content, arrangement and composition compared with two *Benedenia* species. *Mol Biol Rep*. 2014; 41: 6583–6589. <https://doi.org/10.1007/s11033-014-3542-6> PMID: 25024046
33. Huysse T, Plaisance L, Webster BL, Mo TA, Bakke TA. The mitochondrial genome of *Gyrodactylus salaris* (Platyhelminthes: Monogenea), a pathogen of Atlantic salmon (*Salmo salar*). 2007; 739–747. <https://doi.org/10.1017/S0031182006002010> PMID: 17156582
34. Plaisance L, Huysse T, Littlewood DTJ, Bakke TA, Bachmann L. The complete mitochondrial DNA sequence of the monogenean *Gyrodactylus thymalli* (Platyhelminthes: Monogenea), a parasite of grayling (*Thymallus thymallus*). *Mol Biochem Parasitol*. 2007; 154: 190–194. <https://doi.org/10.1016/j.molbiopara.2007.04.012> PMID: 17559954
35. Zhang J, Wu X, Xie M, Li A. The complete mitochondrial genome of *Pseudochauhannea macrorchis* (Monogenea: Chauhanidae) revealed a highly repetitive region and a gene rearrangement hot spot in Polyopisthocotylea. *Mol Biol Rep*. 2012; 39: 8115–8125. <https://doi.org/10.1007/s11033-012-1659-z> PMID: 22544610
36. Kang S, Kim J, Lee J, Kim S, Min G-S, Park J. The complete mitochondrial genome of an ectoparasitic monopisthocotylean fluke *Benedenia hoshinai* (Monogenea: Platyhelminthes). *Mitochondrial DNA*. 2012; 23: 176–178. <https://doi.org/10.3109/19401736.2012.668900> PMID: 22545965
37. Baeza JA, Sepúlveda FA, González MT. The complete mitochondrial genome and description of a new cryptic species of *Benedenia* Diesing, 1858 (Monogenea: Capsalidae), a major pathogen infecting the yellowtail kingfish *Seriola lalandi* Valenciennes in the South-East Pacific. *Parasit Vectors*. 2019; 12: 490. <https://doi.org/10.1186/s13071-019-3711-5> PMID: 31623679
38. Zhang D, Zou H, Wu SG, Li M, Jakovlić I, Zhang J, et al. Sequencing of the complete mitochondrial genome of a fish-parasitic flatworm *Paratetraonchoides inermis* (Platyhelminthes: Monogenea): tRNA gene arrangement reshuffling and implications for phylogeny. *Parasit Vectors*. 2017; 10: 462. <https://doi.org/10.1186/s13071-017-2404-1> PMID: 29017532
39. Zhang D, Li WX, Zou H, Wu SG, Li M, Jakovlić I, et al. Mitochondrial genomes of two diplectanids (Platyhelminthes: Monogenea) expose paraphyly of the order Dactylogyridea and extensive tRNA gene rearrangements. *Parasites and Vectors*. 2018; 11: 1–13.
40. Zhang D, Zou H, Jakovlić I, Wu SG, Li M, Zhang J, et al. Mitochondrial genomes of two thaparocleidus species (Platyhelminthes: Monogenea) reveal the first rRNA gene rearrangement among the neodermata. *Int J Mol Sci*. 2019;20. <https://doi.org/10.3390/ijms20174214> PMID: 31466297
41. Jedličková L, Dvořáková H, Kašný M, Ilgová J, Potěšil D, Zdráhal Z, et al. Major acid endopeptidases of the blood-feeding monogenean *Eudiplozoon nipponicum* (Heteronchoinea: Diplozoidae). *Parasitology*. 2016; 143: 494–506. <https://doi.org/10.1017/S0031182015001808> PMID: 26888494
42. Jedličková L, Dvořák J, Hrachovinová I, Ulrychová L, Kašný M, Mikeš L. A novel Kunitz protein with proposed dual function from *Eudiplozoon nipponicum* (Monogenea) impairs haemostasis and action of complement in vitro. *Int J Parasitol*. 2019; 49: 337–346. <https://doi.org/10.1016/j.ijpara.2018.11.010> PMID: 30796952
43. Ilgová J, Jedličková L, Dvořáková H, Benovics M, Mikeš L, Janda L, et al. A novel type I cystatin of parasite origin with atypical legumain-binding domain. *Sci Rep*. 2017; 7: 17526. <https://doi.org/10.1038/s41598-017-17598-2> PMID: 29235483
44. Ilgová J, Kavanová L, Matiašková K, Salát J, Kašný M. Effect of cysteine peptidase inhibitor of *Eudiplozoon nipponicum* (Monogenea) on cytokine expression of macrophages in vitro. *Mol Biochem Parasitol*. 2020; 235: 111248. <https://doi.org/10.1016/j.molbiopara.2019.111248> PMID: 31874193
45. Fajtová P, Štefanić S, Hradilek M, Dvořák J, Vondrášek J, Jílková A, et al. Prolyl Oligopeptidase from the Blood Fluke *Schistosoma mansoni*: From Functional Analysis to Anti-schistosomal Inhibitors.

- Correa-Oliveira R, editor. PLoS Negl Trop Dis. 2015; 9: e0003827. <https://doi.org/10.1371/journal.pntd.0003827> PMID: 26039195
46. Wiśniewski JR, Zougman A, Nagaraj N, Mann M. Universal sample preparation method for proteome analysis. *Nat Methods*. 2009; 6: 359–362. <https://doi.org/10.1038/nmeth.1322> PMID: 19377485
 47. Cox J, Mann M. MaxQuant enables high peptide identification rates, individualized p.p.b.-range mass accuracies and proteome-wide protein quantification. *Nat Biotechnol*. 2008; 26: 1367–1372. <https://doi.org/10.1038/nbt.1511> PMID: 19029910
 48. Cox J, Neuhauser N, Michalski A, Scheltema RA, Olsen J V., Mann M. Andromeda: A Peptide Search Engine Integrated into the MaxQuant Environment. *J Proteome Res*. 2011; 10: 1794–1805. <https://doi.org/10.1021/pr101065j> PMID: 21254760
 49. Perez-Riverol Y, Csordas A, Bai J, Bernal-Llinares M, Hewapathirana S, Kundu DJ, et al. The PRIDE database and related tools and resources in 2019: improving support for quantification data. *Nucleic Acids Res*. 2019; 47: D442–D450. <https://doi.org/10.1093/nar/gky1106> PMID: 30395289
 50. Kanehisa M, Furumichi M, Tanabe M, Sato Y, Morishima K. KEGG: New perspectives on genomes, pathways, diseases and drugs. *Nucleic Acids Res*. 2017; 45: D353–D361. <https://doi.org/10.1093/nar/gkw1092> PMID: 27899662
 51. Protasio A V, Tsai IJ, Babbage A, Nichol S, Hunt M, Aslett MA, et al. A Systematically Improved High Quality Genome and Transcriptome of the Human Blood Fluke *Schistosoma mansoni*. Hoffmann KF, editor. *PLoS Negl Trop Dis*. 2012; 6: e1455. <https://doi.org/10.1371/journal.pntd.0001455> PMID: 22253936
 52. Konstanžová V, Koubová B, Kašný M, Ilgová J, Dzika E, Gelnar M. Ultrastructure of the digestive tract of *Paradiplozoon homioion* (Monogenea). *Parasitol Res*. 2015; 114: 1485–1494. <https://doi.org/10.1007/s00436-015-4331-4> PMID: 25645005
 53. Brennan GP, Ramasamy P. Ultrastructure of the surface structures and electron immunogold labeling of peptide immunoreactivity in the nervous system of *Pseudothoracocotyla indica* (Polyopisthocotylea: Monogenea). *Parasitol Res*. 1996; 82: 638–646. <https://doi.org/10.1007/s004360050178> PMID: 8875573
 54. Cohen SC, Kohn A, Baptista-farias MFD. Scanning and Transmission Electron Microscopy of the Tegument of *Paranaella luquei* Kohn, Baptista-Farias & Cohen, 2000 (Microcotylidae, Monogenea), Parasite of a Brazilian Catfish, *Hypostomus regani*. 2001; 96: 555–560. <https://doi.org/10.1590/s0074-02762001000400019> PMID: 11391431
 55. Lyons KM. The epidermis and sense organs of the monogenea and some related groups. *Adv Parasitol*. 1973; 11: 193–232. [https://doi.org/10.1016/s0065-308x\(08\)60187-6](https://doi.org/10.1016/s0065-308x(08)60187-6) PMID: 4601372
 56. Konstanžová V, Ka M, Ilgová J, Dzika E, Gelnar M. An ultrastructural study of the surface and attachment structures of *Paradiplozoon* (Monogenea: Diplozoidae). 2017; 1–10. <https://doi.org/10.1186/s13071-017-2203-8> PMID: 28545591
 57. Conn DB. The biology of flatworms (Platyhelminthes): Parenchyma cells and extracellular matrices. *TransAmMicroscSoc*. 1993; 112: 241–261. <https://doi.org/10.2307/3226561>
 58. Pshezhetsky A V. Lysosomal Carboxypeptidase A. *Handbook of Proteolytic Enzymes*. Elsevier; 2013. pp. 3413–3418. <https://doi.org/10.1016/B978-0-12-382219-2.00754-7>
 59. Liu F, Lu J, Hu W, Wang S-YY, Cui S-JJ, Chi M, et al. New perspectives on host-parasite interplay by comparative transcriptomic and proteomic analyses of *Schistosoma japonicum*. *PLoS Pathog*. 2006; 2: 268–281. <https://doi.org/10.1371/journal.ppat.0020029> PMID: 16617374
 60. Horn M, Nussbaumerová M, Šanda M, Kovářová Z, Srba J, Franta Z, et al. Hemoglobin Digestion in Blood-Feeding Ticks: Mapping a Multi-peptidase Pathway by Functional Proteomics. *Chem Biol*. 2009; 16: 1053–1063. <https://doi.org/10.1016/j.chembiol.2009.09.009> PMID: 19875079
 61. Roche L, Tort J, Dalton J. The propeptide of *Fasciola hepatica* cathepsin L is a potent and selective inhibitor of the mature enzyme. *Mol Biochem Parasitol*. 1999; 98: 271–277. [https://doi.org/10.1016/s0166-6851\(98\)00164-9](https://doi.org/10.1016/s0166-6851(98)00164-9) PMID: 10080395
 62. Dvorak J, Horn M. Serine proteases in schistosomes and other trematodes. *Int J Parasitol*. 2018; 48: 333–344. <https://doi.org/10.1016/j.ijpara.2018.01.001> PMID: 29477711
 63. Glerup S, Boldt HB, Overgaard MT, Sottrup-Jensen L, Giudice LC, Oxvig C. Proteinase Inhibition by Proform of Eosinophil Major Basic Protein (pro-MBP) Is a Multistep Process of Intra- and Intermolecular Disulfide Rearrangements. *J Biol Chem*. 2005; 280: 9823–9832. <https://doi.org/10.1074/jbc.M413228200> PMID: 15647258
 64. Jones MK, Higgins T, Stenzel DJ, Gobert GN. Towards tissue specific transcriptomics and expression pattern analysis in schistosomes using laser microdissection microscopy. *Exp Parasitol*. 2007; 117: 259–266. <https://doi.org/10.1016/j.exppara.2007.06.004> PMID: 17662980